Title
Flexible Pressure Sensors for Objective Assessment of Motor Disorders

Journal
Advanced Functional Materials, 30(20)

ISSN
1616-301X

Authors
Amit, Moran
Chukoskie, Leanne
Skalsky, Andrew J
et al.

Publication Date
2020-05-01

DOI
10.1002/adfm.201905241

Peer reviewed

ADVANCED FUNCTIONAL MATERIALS
www.afm-journal.de

Flexible Pressure Sensors for Objective Assessment of Motor Disorders

Q1 *Moran Amit, Leanne Chukoskie, Andrew Skalsky, Harinath Garudadri, and Tse Nga Ng**

Monitoring body motion is relevant to motor control disorders as well as assessment of fine motor skills in child development. Furthermore, motion tracking is necessary for rehabilitation monitoring and injury prevention and benefits both sick and healthy individuals. Flexible pressure sensors based on resistors, capacitors, inductors, or transistors are reviewed in the context of healthcare measurements, ranging from physiological signals to body movement characteristics such as grip and gait. To demonstrate the use of flexible pressure sensors for motor assessment, a touch sensing glove that evaluates fine motor skills in autism research is developed. The results show that autistic children perform fewer taps per minute compared to typically developing children, with larger variations in tap durations. In a second example, a force and motion sensing glove is developed to assess spasticity, a neuromuscular disorder that causes muscle stiffness/resistance and jerky movement. Analyses of force versus velocity show movement-dependent muscle resistance in a patient with spasticity. Through these flexible sensor systems, the shift from subjective scores to objective measurement will promote better diagnosis and dramatically improve the accuracy in tracking patient response to therapy.

1. Introduction

Monitoring body motion offers clues to a person's health status and aging process.[1] Motion tracking studies have provided guidelines to prevent sports injuries[2] and to enhance occupational well-being.[3] Continuous monitoring of body movements can provide feedback on injury rehabilitation[4–6] and enable early detection of disorders that affect motor control, for example, Parkinson's disease and multiple sclerosis.[7,8] Furthermore, assessment of fine motor skills is one of the screening tests for conditions such as epilepsy[9] and autism spectrum disorder (ASD).[10,11] However, the current approach to evaluate motor skills is often subjective; that is, clinicians would observe patients doing certain movements, and then clinicians rank each patient's level according to qualitative descriptions in benchmark classification scales.[12,13] The subjective scores can be inconsistent between raters and do not capture fine-level changes in a patient's progress in response to therapy. Therefore, there is a critical need to tackle the issue of imprecise assessment of motor disorders.

With recent advances in flexible sensors and innovations in tactile sensing,[14–19] we have new low-cost technologies that are prime to facilitate quantitative evaluation of motor control. This progress report presents current developments in wearable sensor systems applicable to motor disorders, so that consistent, objective metrics become available to accurately track whether a treatment effectively relieves symptoms. The wearable sensors are not limited to placement on patients but can also be worn by clinicians or caregivers to assist them in taking measurements during patient interactions.[20,21] The point-of-care sensor systems will allow frequent monitoring, which is highly desirable to offer a better understanding of the patient's short and long-term response to therapies, to tailor treatment and improve outcome and quality of life for patients.

Other reviews[14–19] have already extensively covered the flexible materials and devices used in tracking vital signs and electronic skin applications. In light of that, this progress report focuses on the applications in monitoring motor skills, in particular to implement pressure sensor designs for wearable systems with diverse form factors, for instance, gloves,[20,22,23] epidermal tags tags,[24,25] and shoe insoles.[26,27] We will discuss the mechanisms behind different pressure sensor designs

Dr. M. Amit, Prof. T. N. Ng
Department of Electrical and Computer Engineering
University of California San Diego
Q3 La Jolla, San Diego, CA 92093, USA
E-mail: tnn046@ucsd.edu

Dr. L. Chukoskie
Qualcomm Institute
Research on Autism and Development Laboratory
University of California San Diego
La Jolla, San Diego, CA 92093, USA

Q4 The ORCID identification number(s) for the author(s) of this article can be found under https://doi.org/10.1002/adfm.201905241.

Dr. A. Skalsky
Department of Orthopedic Surgery
University of California San Diego
La Jolla, San Diego, CA 92093, USA

Dr. A. Skalsky
Rady Children's Hospital
San Diego, CA 92123, USA

Prof. H. Garudadri
Qualcomm Institute
University of California San Diego
La Jolla, San Diego, CA 92093, USA

DOI: 10.1002/adfm.201905241

in Section 2, the material choices in Section 3, and healthcare applications based on body motion sensing in Section 4. Specifically, we will show the progress of our own work for two use cases: i) tracking fine motor skills in autism research and ii) quantifying spasticity, a debilitating condition with increased stiffness of the limbs and inability to produce fluid movements as a result of brain injury, stroke, cerebral palsy, and other diseases. We will present our perspectives on sensor designs and limitations and our approaches to engineer systems toward practical clinical use.

2. Sensor Designs and Mechanisms

The transduction of mechanical forces into electrical signals has been realized in flexible devices that measure strain, pressure, torque,[28,29] or acceleration.[30,31] Here we focus our discussions on pressure sensors; but we note that the designs may be generalizable to other mechanical sensor types because strain and stress (i.e., pressure) are connected by elastic moduli, and the forces measured by pressure sensors can be extracted to infer torque or acceleration. We categorize pressure sensing mechanisms into equivalent-circuit components as shown in **Figure 1**, represented by passive components (resistors, capacitors, and inductors) and active amplification devices (transistors). Individual sensor performance metrics, such as the detection limit, sensitivity/resolution, linearity, and response time, are compared across the categories, along with system-level considerations of power consumption and environmental stability. **Table 1** summarizes the main transduction mechanisms, materials, advantages, and limitations for four different types of pressure sensor.

2.1. Resistive Pressure Sensors

Resistive pressure sensors consist of an elastic conductive or a semiconductive layer in contact with two electrodes. The electrodes can be in a coplanar interdigitated geometry (Figure 1a)[32] or they can be vertically aligned as a sandwich structure (Figure 1b).[33] The elastic layer is patterned to tune the elastic modulus; some microstructure examples include sponges,[34] pyramidal structures,[35–37] and nanowires[38,39] which specifically allow sensors to be anisotropic and selectively respond only to a certain pressure direction.[40] Resistance R is given by $R = \rho L/A$, where ρ is the resistivity, L is the length, and A is the cross-sectional area of the elastic layer. In the case of constant resistivity ρ, the dimensional changes in L and/or A under pressure determine the change in R. Alternatively, the resistivity ρ of the elastic layer could vary with pressure. For instance, in a piezoresistive semiconductor the change in band structure under pressure would shift ρ, or in a composite material pressure decreases the interparticle separation distance and thereby reduces ρ. The contact resistance between the electrodes and the elastic layer may be affected by pressure, adding to the change in the overall measured resistance.

Resistive pressure sensors offer wide dynamic range spanning orders of magnitudes, relatively simple device structures and fabrication processes, and a detection limit down to 0.6 Pa.[41] At very low pressure range < 10 Pa, high sensitivity of 44 900% change kPa^{-1} could be reached.[42] Due to their small footprint, resistive sensors can be integrated at high density in pixelated sensor arrays. However, the disadvantages seen in resistive sensors are that they show higher drift over time and are more sensitive to temperature compared to capacitive and inductive devices, when accounting for thermal expansion and thermally induced dielectric constant variation.[43,44] Polymer resistive sensors are limited to slow millisecond response time and display hysteresis between loading and unloading responses because of the viscoelasticity in polymers. The viscoelastic properties affect other sensor mechanisms as well, to be discussed below.

2.2. Capacitive Pressure Sensors

The structures of capacitive pressure sensors can be in a parallel-plate geometry (Figure 1c)[45] or a coplanar form with interdigitated electrodes (Figure 1d).[46] For capacitive sensors the elastic layers between the electrodes are made of insulators, in contrast to (semi)conducting composites in resistive sensors. On the other hand, similar to resistive

Moran Amit received her Ph.D. in materials engineering from the Ben-Gurion University of the Negev in 2015. During 2016 she was a postdoctoral fellow in the Department of Materials Engineering at the Ben-Gurion University of the Negev. In 2017 she joined the University of California San Diego as a postdoctoral fellow in the Department of Electrical and Computer Engineering. Her current research focuses on objective assessment of motor disorders with flexible and wearable sensors.

Tse Nga Ng is an associate professor in the Department of Electrical and Computer Engineering at University of California San Diego (UCSD). Her research focuses on materials and devices in flexible electronics as well as novel fabrication techniques toward additive manufacturing. Prior to UCSD, she was a research scientist at Palo Alto Research Center, a Xerox Company. She received her Ph.D. in physical chemistry under the mentorship of Prof. John Marohn at Cornell University. Q2

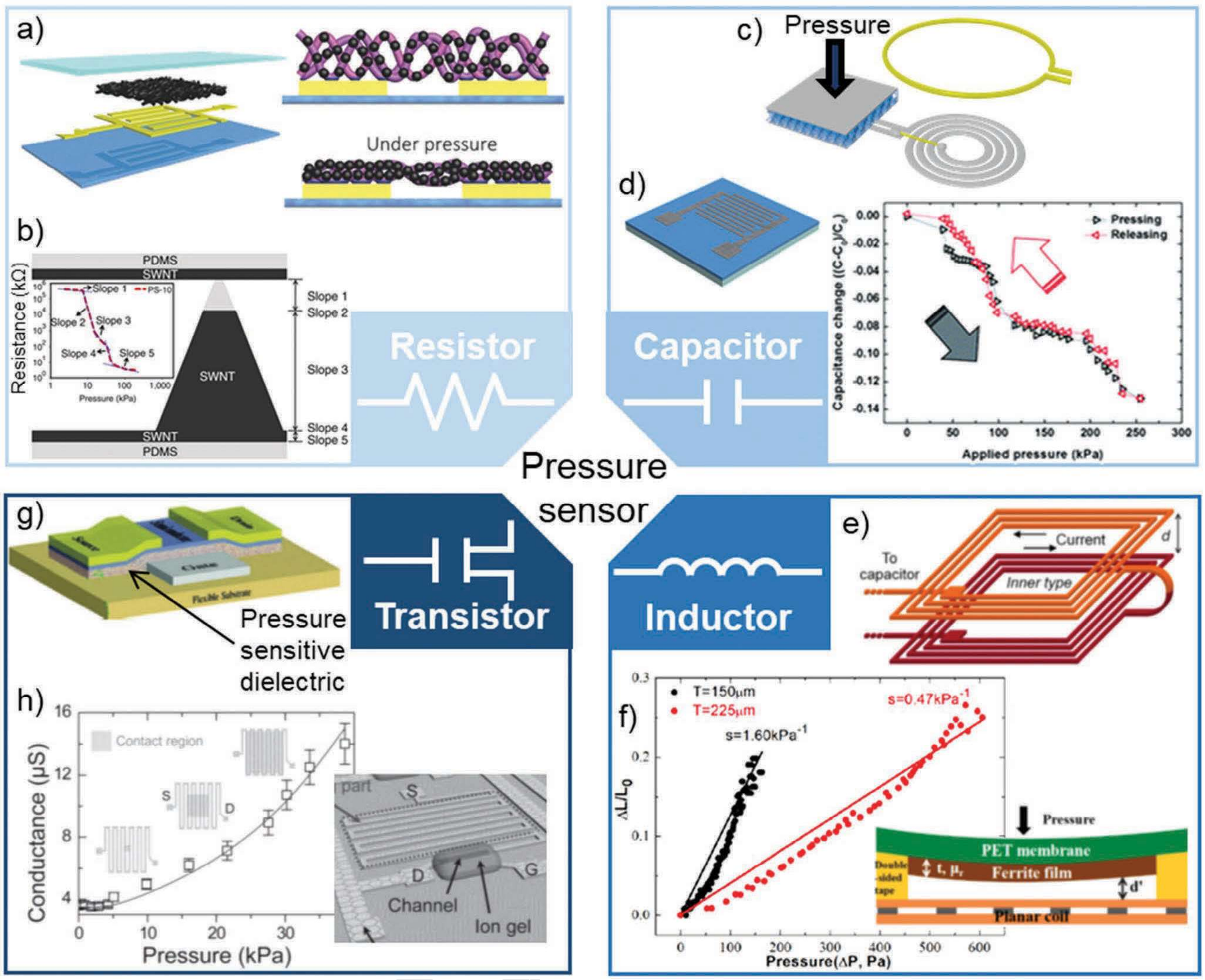

Figure 1. Pressure sensor designs. a) Coplanar interdigitated resistive pressure sensor. Reproduced with permission.[32] Copyright 2015, Wiley-VCH. b) Vertical sandwich structure of resistive pressure sensor with a pyramidal elastomer composite. Reproduced with permission.[33] Copyright 2015, Springer Nature Publishing. c) Parallel-plate capacitive pressure sensor with a fixed inductor to allow wireless communication. Reproduced with permission.[45] Copyright 2018, IOP Publishing. d) Coplanar capacitive sensor scheme. Reproduced with permission.[46] Copyright 2016, The Royal Society of Chemistry. e) Inductive pressure sensor with spiral coils placed on flexible membranes in a folded geometry. Reproduced with permission.[68] Copyright 2009, Elsevier. f) Inductive pressure sensor tuned by a magnetic core material. Reproduced with permission.[69] Copyright 2019, MDPI. g) Transistor-based pressure sensor with a piezoelectric dielectric. Reproduced with permission.[76] Copyright 2011, American Chemical Society. h) Transistor-based pressure sensor with gel dielectric that spreads over a wider area under pressure. Reproduced with permission.[78] Copyright 2014, Wiley-VCH.

sensors, the compressibility of elastic dielectrics is tuned by microstructuring[47–49] and adding air voids,[45,50,51] to lower elastic moduli in capacitive pressure sensors. Hierarchical structures[52] further enhance capacitive sensor arrays to detect the direction of the applied pressure.

The capacitance C is given by $C = \varepsilon_0 \varepsilon_r A/d$, where ε_0 is the permittivity of vacuum, ε_r is the relative permittivity of the material, A is the area of the electrode plates, and d is the distance between the plates. Changes to the geometric parameters (d and A) are major contributors to the capacitance change under pressure in parallel-plate capacitors. Another contribution to the capacitance is from the relative permittivity ε_r of the dielectric composite,[53] which changes as the volume ratio of air to polymer varies under pressure. The coplanar design relies on tuning permittivity and is widely used for capacitive touch sensors,[54,55] which are essentially simplified pressure sensors. When the fringe fields between the electrodes are disturbed by an object, the capacitance is changed to indicate a touch event. The capacitance change due to relative permittivity changes can also be attributed to change in nanoparticles density inside the dielectric layer.[54] It should be noted, that as the capacitive sensors are elastic, dimensional change of the coplanar capacitor could also occur and attribute to the overall capacitance change.[46]

Capacitive sensors exhibit the advantages of low sensitivity to temperature and humidity variations and low power consumption compared to resistors. Pressure sensitivity of 42% change kPa^{-1} for range <1.5 kPa and a detection limit of 1 Pa

Table 1. Pressure sensors mechanisms, materials, advantages, and limitations.

Pressure sensing mechanism	Material of active sensing layer	Advantages	Limitations
Resistive	Conductive or semiconductive	• Wide dynamic range • Relatively simple device structures and fabrication • High sensitivity at very low pressure range • Best detection limit • Can be integrated at high density in pixelated sensor arrays	• High drift over time • More sensitive to temperature changes • Polymer resistive sensors limited by slow response time and hysteresis
Capacitive[a)]	Insulating	• Low sensitivity to temperature and humidity variations • Low power consumption	• Relatively low linear dynamic range • Susceptibility to electromagnetic interference and parasitic coupling to the surroundings • If using polymers, may be limited by slow response time and hysteresis
Inductive	Conductive	• High environmental stability • Enables wireless communication designs	• Larger device footprint • Relatively complex fabrication
Transistor	Insulating, semiconductive, or conductive	• Built-in current amplification • Enable scaling to large-area active-matrix arrays with high spatial resolution	• Drift and bias stress instability • Need for complex optimization of contact resistance and semiconductor transport properties

[a)]Sub-types include piezoelectric and triboelectric pressure sensors.

are reported for microstructured capacitive sensor.[56] The combination of a structured pyramid dielectric layer that is also comprised of porous material resulted in very high sensitivity of 4450% change kPa^{-1} (range < 100 Pa), a detection limit of 0.14 Pa, and was insensitive to a temperature change of up to 100 °C.[42] Yet capacitive pressure sensors show relatively low linear dynamic range and susceptibility to electromagnetic interference and parasitic coupling to the surroundings. The response time and hysteresis may be limited by viscoelastic polymer dielectrics. Nonetheless, for two sub-types of capacitive transducers—piezoelectric or triboelectric sensors, they offer fast response time and can operate as energy-harvesting devices.

2.2.1. Piezoelectric Pressure Sensors

Piezoelectric capacitors use piezoelectric materials as the dielectric. The piezoelectric materials produce a voltage proportional to the applied pressure, due to breaking of symmetry in the chemical structure by external forces.[57–59] The equivalent circuit model of a piezoelectric pressure sensor consists of a capacitor in series with a voltage source dependent on pressure.[60] Common piezoelectric polymers, such as polyvinylidene fluoride and its derivatives, have demonstrated fast microsecond response time, high sensitivity of 14 V kPa^{-1}, and a detection limit of 15 Pa.[58] On the other hand, these materials are temperature sensitive, and the generated voltage dissipates under static conditions. Thus, piezoelectric sensors are suitable for measuring dynamic stimuli but not for monitoring constant pressure.

2.2.2. Triboelectric Pressure Sensors

Triboelectric pressure sensors are based on contact electrification and electrostatic induction;[61–63] namely, they use mechanical rubbing between insulators to induce charges on electrodes. The electrostatic charges generated by periodic contact and separation of two insulator surfaces produce an alternating potential and current. A wide variety of triboelectric device structures are available through simple fabrication, as insulating thin polymer films on electrodes are mounted in configurations that draw on mechanical friction.[57,64–66] A triboelectric device is represented by a voltage source, which originates from the separation of the charges, in series connection with a capacitor, which originates from the capacitance between the two surfaces.[67] Self-powered triboelectric pressure sensors have been shown to detect pressure from as high as 450 kPa down to 5 kPa with a sensitivity of 0.5 V kPa^{-1}.[66] The main limitation is that triboelectric sensors cannot monitor a constant pressure, as they produce electrical signal only under movement from pressure changes.

2.3. Inductive Pressure Sensors

The structures of inductive pressure sensors use planar spiral coils, placed on flexible membranes in a folded geometry (Figure 1e)[68] or close to a core material (Figure 1f)[69] that changes the coil inductance under pressure. The inductance expressions for spiral inductors are highly dependent on the selected shapes (square, hexagonal, circular, etc.), and we refer readers to ref. [70] for numerical and analytical solutions. In general, the total inductance L has a fixed self-inductance component and a pressure-variable component that is the mutual inductance, which depends on the gap space between the conductor segments or between the coil and a nearby metal core plate. In the case with a magnetic core material like ferrite, the coil inductance is also modulated by changes in effective permeability, as the magnetic core moves toward the coil under pressure.[69,71–73]

Inductive pressure sensors show high environmental stability since the materials are inert conductors and substrates, and they enable wireless designs. An example shows good sensitivity of 160% change kPa^{-1} below 180 Pa and a detection limit of 14 Pa.[69] Inductive coupling allows wireless communications between the sensor circuit and the readout system that measures the sensor resonance frequency. The full sensor circuit is an LCR oscillator with resonance frequency $f = 1/(2\pi\sqrt{LC})$. The sensor can be an inductor or a capacitor component, such as combinations[45,74] of a pressure-sensitive capacitor with a fixed inductor or vice versa. The use of pressure-sensitive inductor is not as common as resistive and capacitive sensors, presumably because of larger device footprint and more complex fabrication incorporating magnetic materials or multiple layers of support structures.

2.4. Transistor-Based Pressure Sensors

Thin-film transistors (TFTs) can serve as sensors converting input pressure to output current. Based on the gradual channel approximation model, the TFT current–voltage characteristics operating in the linear regime is described by $I_{SD} = (W/L)(\mu C)[(V_G - V_T)V_{SD} - V_{SD}^2/2]$, where I_{SD} is the source–drain current, W is the channel width, L is the channel length, μ is the effective carrier mobility, C is the dielectric capacitance, V_T is the threshold voltage, and V_G and V_{SD} are the control gate voltage and the source–drain voltage, respectively. To turn a TFT structure into a pressure sensor, the gate dielectric is modified with pressure-sensitive materials, using strategies such as microstructured insulators[47,75] or composites with piezoelectric particles (Figure 1g)[76] for which the dielectric capacitance C changes under pressure. There is also a suspended flexible polyelectrolyte dielectric structure[77] that modulates the gate capacitance in response to pressure. Another approach modulates the channel ratio W/L, as the gel dielectric spreads over a wider area under pressure (Figure 1h).[78] In addition, the resistance between the source and drain electrodes has been tuned under pressure by using a conductive rubber to vary the transistor current.[79]

TFTs are essential for pixel addressing and TFT-based pressure sensors are integrated structures that enable scaling to large-area active-matrix arrays with high spatial resolution for obtaining pressure maps.[80] This type of sensors has reached sensitivity of 102% change kPa^{-1}.[58] There is built-in current amplification in TFT sensors dependent on the applied V_G and V_{SD} biases, providing a knob to tune the current gain in exchange with power consumption. The caveats with using integrated TFT pressure sensors are that stability issues[81,82] of TFTs may introduce drift in pressure measurements and significant engineering efforts are needed to optimize TFT contact resistance[83] and transport properties.[84]

3. Sensor Materials

A suite of materials ranging from conductors, semiconductors, to insulators are developed to achieve flexibility and stretchability in wearable health monitors.[85] **Figure 2** summarizes our view of the common approaches to simultaneously optimize mechanical and electronic characteristics.

Highly elastic and stretchable conductive materials are needed for the electrodes and interconnects. Examples include composite percolation networks[86,87] of conductive particles and elastomers (Figure 2a), and inherently stretchable materials (Figure 2b) such as liquid eutectic metals[88,89] or conducting polymers[90] demonstrated to maintain a conductivity ≈100 S cm^{-1} under 800% tensile strain. Thin film metals have been made into highly conformal, stretchable conductors by geometry optimization using serpentine[91,92] or cilia structures (Figure 2c).[93]

Semiconducting materials (Figure 2d–f) are essential in current-modulation switches, ranging from transistor-based sensors to bioinspired synaptic devices.[94,95] 1D carbon nanotubes[96] and atomically thin 2D materials[97,98] have been integrated as semiconductors in flexible transistors. Semiconducting polymers with dynamic hydrogen bonds enable robust transistors that are stretchable and repairable by solvent and thermal treatments.[99]

Electrical insulators constitute the dielectrics in capacitors, inductors, and transistors. Many elastic polymers are available and their mechanical moduli are easily tunable by varying crosslinker ratios and hydrogen bonding like in hydrogel[100] (Figure 2g).[100] Particular properties such as piezoelectric responses[101] can be incorporated using a polymer composite with ferroelectric perovskite particles or a ferroelectric polymer such as polyvinylidene fluoride (Figure 2h). The internal structures of dielectrics are often patterned to modify the mechanical modulus for the targeted pressure range (Figure 2i).

In addition to electrical and mechanical properties, other criteria to consider when choosing materials for wearable sensors include the materials processing requirements and safety for human use. As many of the aforementioned polymers and composites are processable as solutions, they are conducive to low-cost printing fabrication[102–106] to make sensors widely deployable. The materials nontoxicity and biocompatibility is a crucial requirement, since pressure sensors for monitoring motor disorders require contact with the human body. Currently sensors are encapsulated with biocompatible materials[107] to interface between the sensor and the human body. In order to minimize electronic waste buildup and reduce environmental impacts, biodegradable materials, such as paper-based pressure sensors,[108,109] could be disintegrated in solution (e.g., phosphate buffer solution) or by incineration. By choosing materials that combine biocompatibility and biodegradability, a class of bioresorbable materials have been used in implanted transient pressure sensors that are safely broken down inside the body, eliminating the need for invasive removal procedure.[110,111]

To achieve durable sensors, self-healing materials that are capable of repairing mechanical fractures autonomously under ambient conditions are desired, particularly for flexible pressure sensors that undergo continuous mechanical deformation during their usage.[112–114] The self-healing mechanisms are categorized as either intrinsic or extrinsic.[112,115] Intrinsic self-healing materials is based on molecular interactions between crosslinking groups embedded onto the polymer chains. They display fast healing times and multiple healing cycles but require extensive molecular designs and synthesis. Extrinsic self-healing materials are based on monomers and catalysts prepacked in capsules or vessels that are released when the

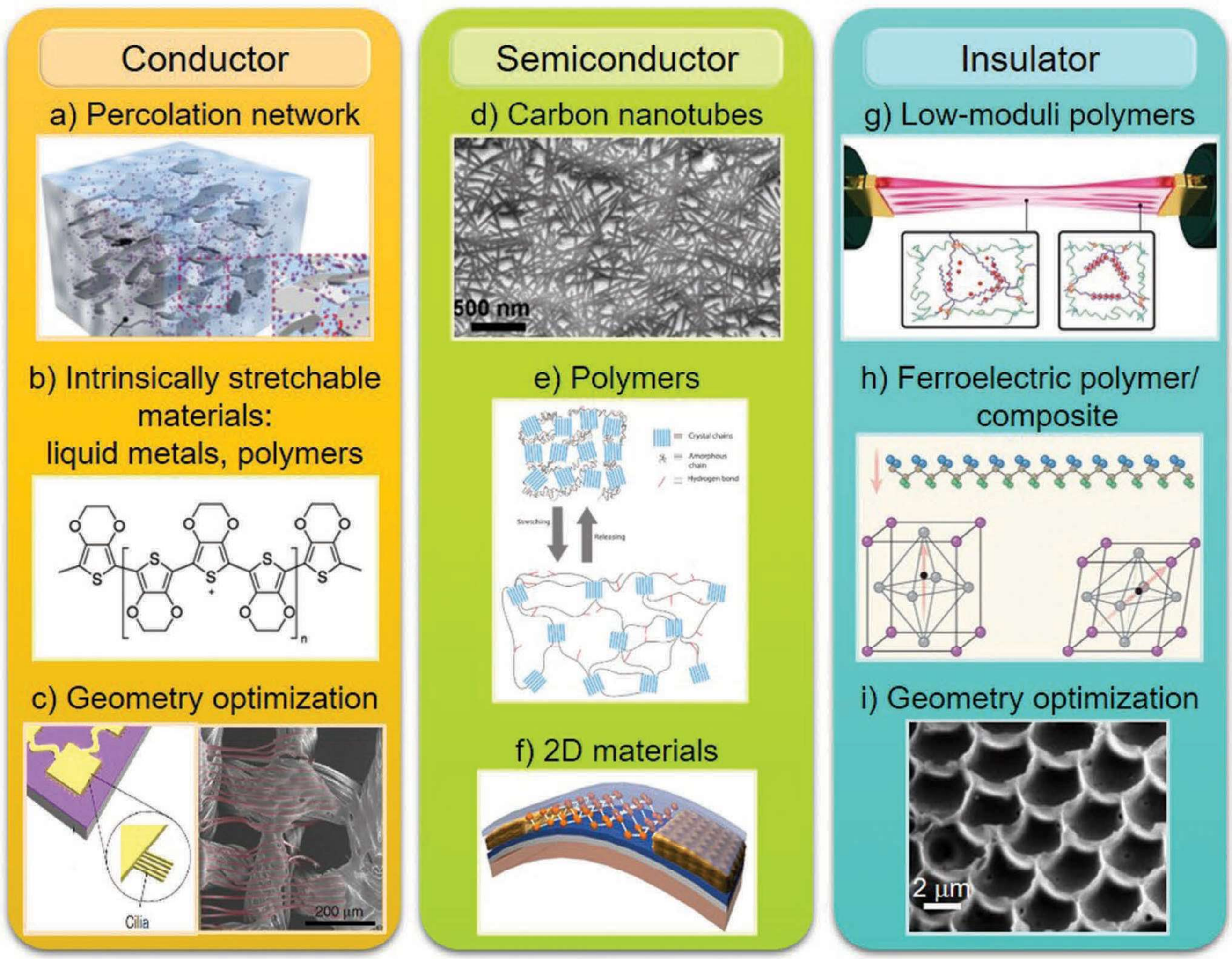

Figure 2. Material choices for flexible pressure sensors. a) Composite percolation network that forms conducting paths with Ag flakes. Reproduced with permission.[86] Copyright 2017, Springer Nature Publishing. b) Chemical structure of poly(3,4-ethylenedioxythiophene), a conducting polymer. c) Metal patterned with cilia to form stretchable structures. Reproduced with permission.[93] Copyright 2016, Springer Nature Publishing. d) Single-walled carbon nanotubes. Reproduced with permission.[166] Copyright 2013, American Chemical Society. e) Schematics of semiconducting conjugated polymers with dynamic hydrogen bonds to improve stretchability. Reproduced with permission.[99] Copyright 2016, Springer Nature Publishing. f) 2D semiconductor. Reproduced with permission.[167] Copyright 2015, American Chemical Society. g) Low-moduli, highly stretchable hydrogel. Reproduced with permission.[100] Copyright 2017, American Association for the Advancement of Science. h) Chemical structure of poly(vinylidene fluoride-*co*-trifluoroethylene) (top) and lead zirconate titanate (bottom). Reproduced with permission.[101] Copyright 2018, Springer Nature Publishing. i) Polyurethane patterned into nanoneedle structures for a dielectric layer. Reproduced with permission.[47] Copyright 2012, American Institute of Physics.

polymer matrix is damaged. They enable large-volume self-healing, yet display slower healing times, and can be more complex to process than intrinsic self-healing materials.

4. Applications of Pressure Sensors in Monitoring Body Motion

Here we categorize body pressure measurements into two ranges in **Figure 3**: i) internal body pressure corresponding to physiological signals, e.g. heart pulse, intraocular pressure, around 15–180 mmHg (≈2–24 kPa); ii) external pressure exerted in motor control studies, exceeding 180 mmHg (>24 kPa) in grip or gait signals. In Sections 4.1–4.3, we present some of the research achievements in flexible wearable electronics. While these prior work discussions are not comprehensive, they provide the context leading to our own work presented in Sections 4.4 and 4.5.

4.1. Monitoring Internal Body Pressure

Flexible pressure sensors have been widely deployed for continuous monitoring of vital signs (e.g., heart rate and respiratory rate) and other physiological signals (e.g., blood pressure and intraocular pressure). The devices have been placed as implants directly inside the body (Figure 3a)[116] or noninvasively outside the body (Figure 3b).[25] Cardiovascular diseases

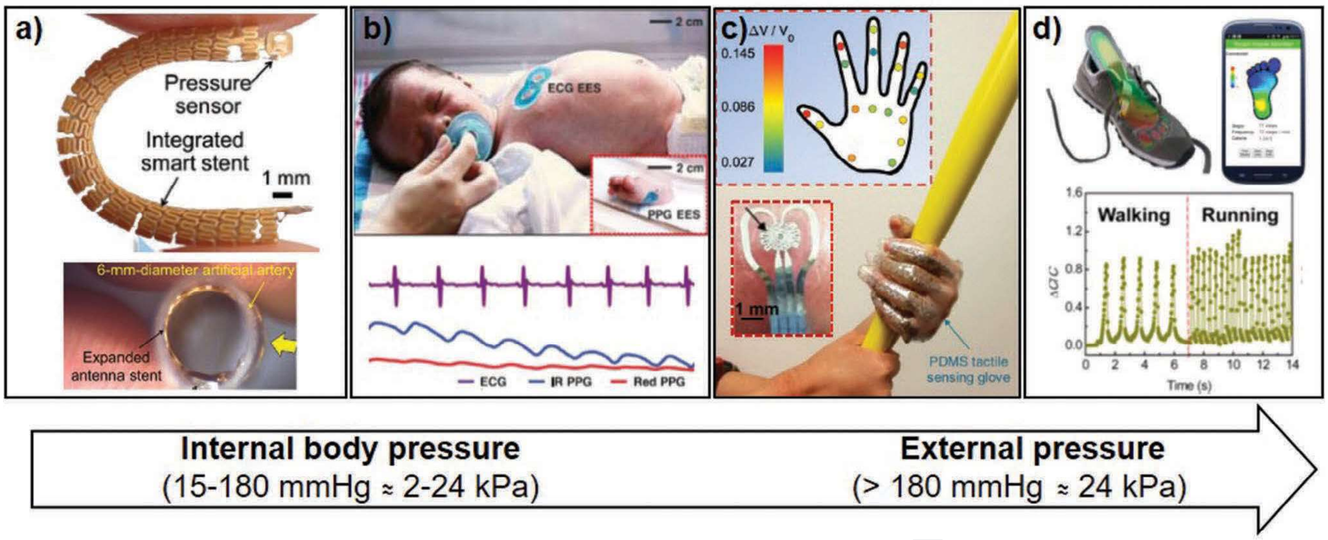

Figure 3. Devices for monitoring body motions. a) Stent with capacitive pressure sensors to monitor blood flow. Reproduced with permission.[116] Copyright 2018, Wiley-VCH. b) Epidermal ECG and PPG sensors. Reproduced with permission.[25] Copyright 2019, American Association for the Advancement of Science. c) Tactile sensing glove measuring grip pressure. Reproduced with permission.[123] Copyright 2017, Wiley-VCH. d) Insole with capacitive pressure sensors. Reproduced with permission.[50] Copyright 2016, American Chemical Society.

are the main cause of mortality worldwide, and especially in people with stents to treat artery obstruction, close monitoring of the blood flow is important to prevent heart attacks and strokes. The stents used to widen arteries will become narrow over time due to endothelial tissue growth or deposits. Thus, a study on stent technologies has incorporated microscale capacitive pressure sensors with wireless interface for in vivo continuous monitoring to detect flow obstruction (Figure 3a).[116] In another example of continuous monitoring based on implants, the intraocular pressure, i.e., the fluid pressure inside the eye, was monitored wirelessly by an *LC* resonator sensor.[117] The intraocular pressure is a primary indicator of glaucoma, the second leading cause of blindness. Sensors that offer wireless, continuous measurement are crucial because peaks in intraocular pressure might occur during sleep time, and not necessarily during daytime checkup.[118] A flexible bioresorbable piezoresistive sensor implant was used to monitor physiological forces in vivo in mice.[110] The system monitored the diaphragmatic contractions to detect breathing patterns, while avoiding invasive removal procedure of the implant.

Changes in internal body pressure are transmitted to the body surface, and noninvasive monitors are capable of inferring many different physiological signals, offering unintrusive health tracking not just for the sick but applicable to wide populations. For example, to avoid surgeries required with implants, flexible sensor technologies are being developed for contact lenses to measure intraocular pressure and detect eye problems.[119,120] Surface measurements of arterial pulse waves that are indicative of the heart health were demonstrated with different pressure sensors, such as a triboelectric sensor[65] or a liquid-capsule platform with a resistive sensor.[121] In another use case, muscle vibrations from the vocal cord were recorded using triboelectric pressure sensor or hydrogel resistive sensor.[65,122] These signals have applications in Parkinson's disease monitoring, as studies found deterioration in phonation due to Parkinson's disease.[7]

4.2. Monitoring Pressure Exerted by Body Movement

Large-area flexible pressure sensor arrays have been integrated into portable systems with high spatial resolution for research in musculoskeletal biomechanics. For instance, grip and gait are common measurements used in therapy and rehabilitation as well as for sports training. Gloves were embedded with resistive sensors for tactile mapping of human grasps.[23] Figure 3c shows hand-grip mapping with microfluidic diaphragm pressure sensors.[123] These resistive diaphragm sensors exploit a Wheatstone bridge circuit to measure tangential and radial strain. Under an applied pressure, a decrease in the tangential cross-sectional area due to tension leads to an increase in the tangential bridge resistance; on the other hand, compression around the periphery results in an increase in the radial cross-sectional area, leading to a decrease in the radial bridge resistance. When the glove is worn by a patient, the grip data indicate upper body and overall strength of the patient.[124] Alternatively, a physician wearing the instrumented glove[20] would be equipped to track forces from different maneuvers while interacting with the patient.

Quantifying plantar pressure using unintrusive, flexible insoles (Figure 3d)[50] provides information regarding gait and posture, which are used for diagnostics in many areas including orthopedic problems, neurological disorders (e.g., multiple sclerosis and Parkinson's disease), sport biomechanics, and injury prevention and rehabilitation.[4,27,125,126] A resistive pressure sensor for monitoring gait uses hydrogels with self-healing capability to extend the sensor life time.[114] Within gait monitoring and analysis research, there is an urgent need to serve diabetic patients by identifying and preventing high pressures on the soles of their feet. The high pressure points would result in ulcerations, and their relief is important to not exacerbate sore spots. Hence, real time monitoring during daily activities is highly desirable to manage such chronic problems.[127]

4.3. Multimodal Monitoring Systems

Multimodal systems that combine several sensors types provide comprehensive analyses for vital signs,[25] chemical biomarkers,[128,129] and musculoskeletal conditions.[5] Comparing pressure signals from arterial pulses and electrocardiograms[130] (ECGs) enable extraction of pulse transit times to determine the systolic blood pressure.[121] Alternatively, the blood flow motion during heart beats can be monitored indirectly in photoplethysmograms[131–133] (PPGs) which use flexible photodetector technologies.[134–137] Notably, a complete epidermal system that allows wireless, battery-free, continuous sensing of PPGs and ECGs on neonates has been achieved with performance comparable to clinical-grade monitoring systems (Figure 3b).[25] Flexible bioresorbable implants that eliminate the need for a second surgery to remove them from the body were demonstrated in vivo on rats to monitor the electrocorticography (ECoG) and intracortical pressure signals.[111] The implanted sensors recorded dynamic changes in brain signals for different stages of epilepsy and simultaneously tracked swelling of the cortex during and after the operation.

The combination of pressure sensors with inertial measurement units[138,139] records parameters of force, power, and range of muscle movements, in order to gather complementary descriptions of motor characteristics in biomechanic studies. Moreover, the use of multimodal sensors has been extended to behavioral studies in child development research. Simultaneous monitoring of body movements and physiological status has been carried out to track stressor response[140] and then predict imminent aggression in children with autism spectrum disorder.[141] Wearable sensor systems that facilitate similar automated tracking would benefit individualized, real-time interventions in the future.

4.4. Objective Assessment of Fine Motor Skills in Children with Autism Spectrum Disorder

4.4.1. Motivation

Our first application example focuses on evaluating fine-motor skills to identify sensory-motor dysfunction, a symptom of neurological disorders (e.g., Alzheimer's, Parkinson's, epilepsy, and autism). The routine screening method used in clinical settings is the finger tapping test (FTT).[142] This simple test scores the number of taps per minute by a patient tapping one's finger on the thumb or on a counter key. The average number is a measure of motor speed. The performance difference of an individual over time can track disease progress or regression.[143] Currently FTT is done by manual counting or is recorded by video camera to be later processed by computer vision algorithms (**Figure 4**a). There are also computer interface devices for FTT,[142,143] but the existing button interface is isolated and not designed for combination tests that examine coordinated motor and cognitive functions. Thus, FTT can be improved by a hardware redesign using flexible sensors.

Specifically, we designed a low-cost (USD$ < 20), intuitive touch sensing glove that can be modularly integrated with tests

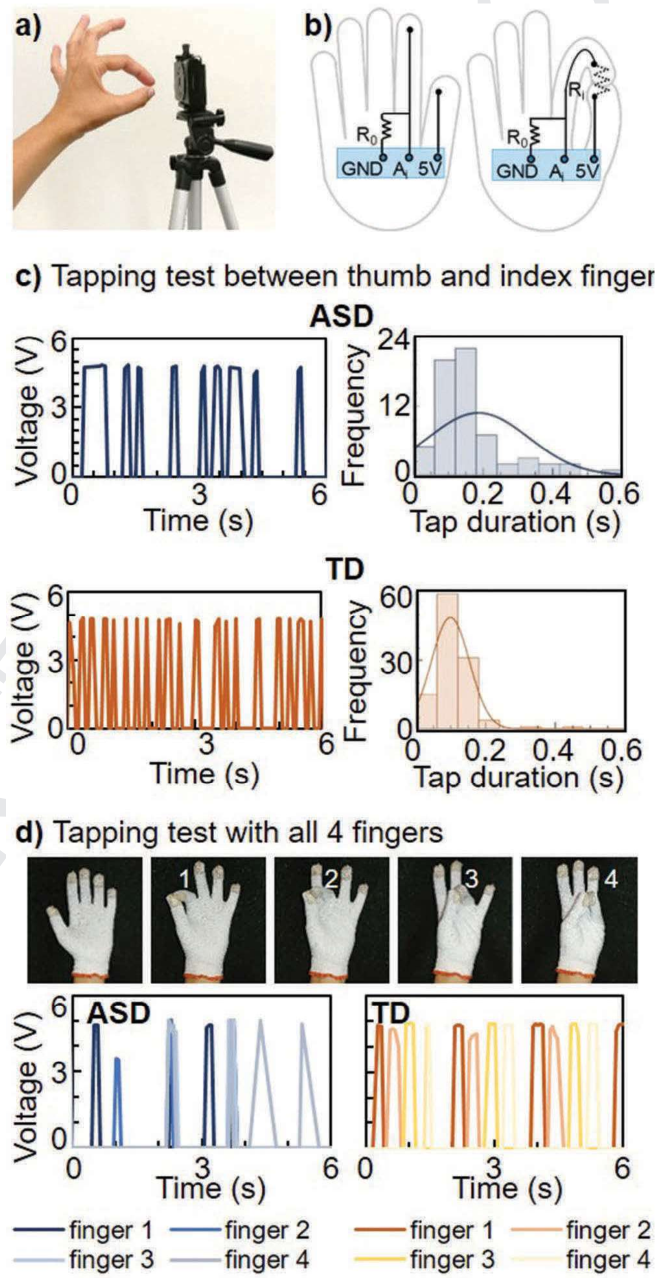

Figure 4. Finger tapping test for evaluating fine motor skills. a) Test recorded by video camera. b) Circuit schematics of the resistive touch sensor glove, with fingers not in contact (left) or in contact (right). c) Representative data of a tapping test between the thumb and the index finger. When fingers are in contact, the signal is high around 5 V; if not in contact, the signal is low at 0 V (left). Corresponding histograms of the contact duration (right). d) Photograph of the contact sequence in a tapping test using all fingers. Representative data showing contact frequency and duration for each finger. Tests here done by children with autism spectrum disorder (ASD) or in typical development (TD).

Q6

that evaluate motor skills and cognition.[144] This glove is used for research in ASD, a common neurodevelopmental disorder that occurs in 1 out of every 68 children and affects ≈1% of the general population. ASD is characterized by deficits in social communications and interactions, as well more commonly overlooked but also important, motor skill deficits, and repetitive behaviors.[11,145–147] Early, accurate identification of motor skill deficits is critical for providing timely intervention treatments that help both the physical and the psychological development of children with ASD. Often their motor skill assessment is done only by observation and questionnaires, which are limited in scope and subjective. Incorporating neuropsychological tests like FTT has helped to objectively characterize movement issues in ASD children and FTT would provide outcome measures to evaluate motor-based interventions.

4.4.2. Measurement Methods and Results

Our resistive touch sensing glove for FTT was made by modifying a fabric glove, on which we patterned conductive electrodes using silver paste[130] or conductive fabric (Sparkfun). The electrodes on finger tips were connected by sewing conductive threads to a microcontroller board (Arduino Nano) sewn at the base of the glove and then packaged up for better user experience.[148] If needed, the resistive touch sensor can be easily modified to integrate pressure sensing function, but for this demonstration the device was made as simple as possible. The electrodes and interconnects could be stretched to about 150% of their original value; this stretchability was sufficient to allow putting the glove on and off without damaging it, and it allowed different test subjects with different hand sizes to wear the same glove. The touch readout used a voltage divider circuit between the thumb and each of the four fingers (index, middle, ring, and pinky), with $R_0 = 510\ \Omega$ and $R_1 = 10\ \Omega$ (Figure 4b). When fingers were in contact, the signal was high around 5 V; if not in contact, the signal was low at 0 V. Our user interface code provided real-time data analysis.

Two types of FTTs were carried out to compare the tapping patterns of ASD and typically developing (TD) children: index-finger tapping test and all-finger tapping test. Three children aged 6–13 in each category was recruited for the first and two children in each category for the latter test. All participants signed an informed consent sheet verified by the University of California San Diego (UCSD) Human Research Protections Program under Institutional Review Board #171587. In the index-finger tapping test, subjects were asked to tap their index finger and the thumb together as many times as possible in a given time interval of 30 s. ASD children performed fewer tap counts than TD children, as seen from the frequency axes of the histograms in Figure 4c. In addition to counts per second, the contact duration was longer and showed more variance for ASD children in comparison to TD children. There was no statistically significant different between measurements with and without the glove (analyzed from video recording), attesting that wearing the glove did not impair finger tapping motion.

In the all-finger tapping test, the subjects were asked to touch their thumb with one finger at a time in sequence as shown in Figure 4d, performing as fast as possible in a given time frame of 30 s. The results of the all-finger tapping test showed irregular tapping pattern by ASD children, as well as events when multiple fingers touching the thumb together at the same time. In contrast, TD children were able to regularly repeat the intended tapping pattern.

The motor deficits in ASD population are being addressed by game-based trainings,[149] and FTTs were part of the toolset to monitor individual progress due to medication or training, and not only for comparison between groups of subjects. Our simple, low-cost touch sensing glove have been incorporated into multitask experiments, for example simultaneously quantifying FTT, balance, and working memory in ASD.[144] The touch sensor is modular and can be adapted to different research tests such as measuring reaction time and touch sequence, as the subject performs tasks while wearing the unintrusive sensor glove. As the fabrication cost is very cheap, it could be widely distributed for clinical studies of motor disorders and monitoring fine motor skills.

4.5. Objective Assessment of Spasticity

4.5.1. Motivation

Our second application example focuses on the assessment of spasticity. Spasticity is a neuromuscular disorder due to brain or nerve damage in patients suffering from cerebral palsy, stroke, etc.[150–152] Spasticity results in muscle stiffness, painful contractures, and jerky limb movements, affecting a person's motor control in balance, gait, eating, hygiene situation, and more. It is estimated that over 12 million people worldwide suffer from some level of spasticity.[151] Timely evaluation and treatment are important to relieve pain and muscle deformities (**Figure 5**a, top), but there is a key problem of imprecise assessment.

An objective, consistent metric is critical for inspecting whether a therapy effectively relieves symptoms. Yet current clinical practice relies on perception. Clinicians would assess patient severity by performing standardized maneuvers,[13,150] in which the clinician extend and flex the patient's affected muscles to gauge the muscular resistance to movement. Based on subjective perception, the clinician scores the muscle condition against benchmark scales, the most common being the Modified Ashworth Scale with only six rating levels (Figure 5a, bottom).[153] This subjective score is not sensitive and known to be inconsistent between raters and even for the same rater.[12,13] Besides inaccuracy, such evaluation requires appointments and are done weeks apart, and the treatment decisions are often lagging, especially affecting development in rapidly growing pediatric patients.

There is ongoing research aiming to better quantify spasticity. Surface electromyography (EMG) was demonstrated to capture the involuntary muscle activations in patients' limbs.[154–156] While the neural signals objectively characterize reflex thresholds, there is no clear relationship that correlates the bursts of neural activities to severity levels of spasticity.[154,157] EMG suffers from low signal reproducibility due to variations in electrode locations, patients' sweating, and

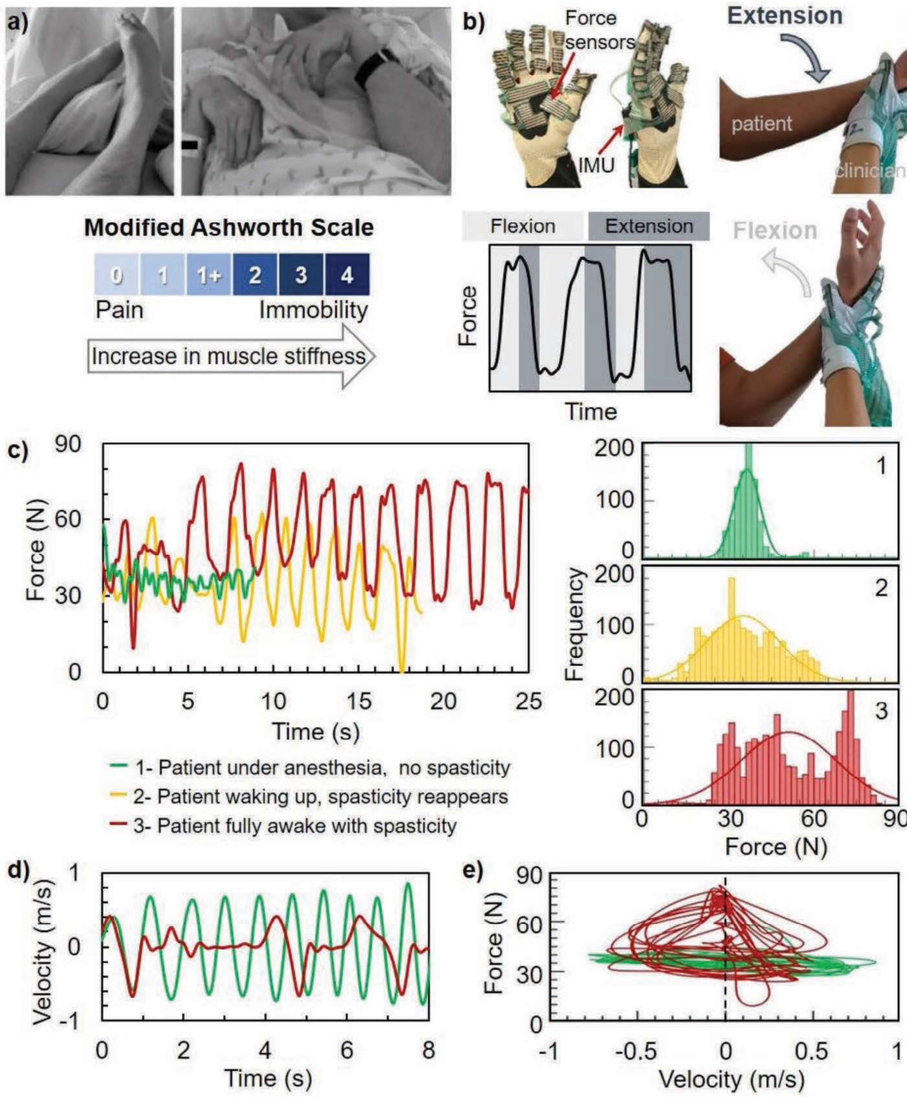

Figure 5. Objective assessment of spasticity. a) Photographs of affected limbs due to spasticity (Reproduced with permission.[168] Copyright 2013, Taylor and Francis.). Benchmark scale commonly used in spasticity evaluation. b) Photographs of our instrumented glove with resistive force sensors and inertial motion unit (IMU). A clinician wears the glove to move a patient's limb into an extension or flexion position. The inset shows a typical force signal measured for multiple extension and flexion cycles. c) Force versus time (left), for three different levels of spasticity in a patient transitioning from being under anesthesia to the fully awake state. Corresponding histograms of force in each state (right). Legend applies to parts (c)–(e). d) Velocity versus time, measured simultaneously with the force data in part (c). e) Force versus velocity.

environmental noise interference. In a different approach, biomechanical devices were developed to measure the muscle stiffness and the peak torque of spastic limbs.[158,159] A six-axis robotic arm was used to manipulate a person's limb and precisely record the position and force to extract resistance of the muscle.[160] However, large motorized structures[160,161] are expensive, complex to operate, and pose safety and clinical adoption barriers. Recently, a compact device was demonstrated to concurrently record muscle torque and EMG.[162,163] Most modules place instrumentation on the patient. In contrast, we design our equipment to be worn by clinicians or caregivers, because it is more reliable to cater the device size to a rater than to various patients, and there is no hardware on patients that may impede movement.

4.5.2. Measurement Method and Results

To address the need for objective assessment of spasticity, we integrate an instrumented glove,[20] equipped with resistive pressure sensors from Tekscan[164] and an inertial motion unit (IMU) from MotionNode. The sensor glove is intended to be worn by the rater, to record the applied force and motion as the rater moves a patient's limb in extension and flexion cycles (Figure 5b). Signals from the pressure sensors are multiplied by active areas and summed together to extract the applied force. The IMU signals, including acceleration, angular velocity, and magnetic field orientation, provide information to extract movement trajectories. Simultaneous force and motion measurements are essential to fully capture the dynamic stiffness/resistance of spastic muscles, since spasticity is perceived to depend on movement velocity and shows catch-and-release symptoms.[165] Below we show data measured by our sensor glove on a patient's spastic knee joint muscles. All measurements were undertaken with patient consent and approved by UCSD Institutional Review Board #180115.

A patient with spasticity underwent a surgical procedure that required general anesthesia. After surgery, the spastic muscle resistance was measured three times: 1) when the patient was under anesthesia, 2) when the anesthesia wore off and patient was waking up, and 3) when the patient was fully awake. As a neuromuscular disorder, spasticity is correlated to one's neural state; it is known that anesthesia would reduce muscle resistance because it decreases neural misfirings. Figure 5c shows the cyclical force exerted to maneuver the patient's joint muscles for several extension and flexion cycles. With the patient under anesthesia, the average force was the lowest at $F_{\text{average}} = 37 \pm 5$ N, and the force histogram distribution was the narrowest among the three measurement states. As anesthesia wore off, force distribution became wider with $F_{\text{average}} = 35 \pm 13$ N. The peak-to-peak force increased, indicating higher muscle resistance. When the patient was fully awake, the average force increased significantly at $F_{\text{average}} = 51 \pm 17$ N, accompanied by a change in force distribution, which will be clarified by the velocity discussion below.

Figure 5d shows large difference in movement velocities between states 1 and 3. The linear velocity was converted from the angular velocity acquired from IMU gyroscope along the direction of movement, multiplied with the distance between the rater's grip and the patient's knee joint. Under anesthesia, the patient's muscle was easy to flex and extend, and the velocity was highly cyclical as shown by the green data. When spasticity became more prominent after anesthesia wore off, the recorded velocity was no longer cyclical, because the patient's limb could not be moved fluidly as shown by the red data.

Analysis of the combined signals, i.e., force as function of velocity in Figure 5e, attests that spasticity is motion dependent. The maneuver force was independent of movement velocity for state 1 (green data). In state 3, the force required to move spastic muscle increased, particularly as velocity was near zero when the rater switched between flexion and extension (red data). It should be noted that for the patient examined here, the force–velocity relationship was not symmetric between flexion (i.e., positive velocity) and extension (i.e., negative velocity). Indeed, for some patients their muscle resistance is more noticeable in one segment of the maneuver cycle and less in the other. As the next step, we will explore additional parameters to describe spasticity, such as the range of motion and the expended power.

Overall, the significance of the above measurements is that our multimodal sensor glove can clearly distinguish changes in muscle spasticity and is promising for quantifying spasticity. It will enable a point-of-care device that allows frequent evaluation by caregivers. The shift from subjective scores to objective measurements will promote better diagnosis and dramatically improve the accuracy in tracking patient response to therapy.

5. Summary and Future Outlook

Flexible pressure sensors facilitate objective assessment of motor disorders. In particular, we have demonstrated their use in two cases. In the first example we used resistive touch sensors to quantify finger tapping patterns of autistic children. In an index tapping test ASD children performed less counts per minute, with larger tap duration and larger variation in the tap duration, compared to TD children. In all-fingers tapping test the ASD children had irregular patterns compared to TD children and tended to skip fingers more often. This touch-sensing glove could be used in combination with other tests and for other conditions that require neuropsychological assessment of fine motor skills via finger tapping tests, such as Parkinson's disease, stroke, and epilepsy. Its computer interface could be used in the future for gamification purposes, to use it for fine motor skills training.

In the second case we demonstrated a multimodal sensor glove, to be worn by clinicians for measuring spasticity. The average applied force and its distribution increased, indicating higher muscle resistance, as anesthesia wore off a patient with spasticity. In addition, the limb movement was tracked and shown to be less fluid with spasticity. The analysis of force versus velocity clearly showed a difference in the level of spasticity between flexion and extension maneuvers. This novel wearable system will enable accurate diagnosis and effective evaluation of intervention outcomes, toward improving care and quality of life for patients with spasticity. Moreover, the instrumented glove could be used in a wide range of clinical procedures that are currently based on perception of motion and force, and in other studies on musculoskeletal rehabilitation.

Objective assessment of motor disorders is an interdisciplinary effort. The basic pressure sensing principles open the door to many possible applications that target various healthcare problems and provide physiological information. The next steps for objective motion characterization are developments in signal processing to extract key information out of noisy real-life data, in addition to improvements in sensor design and data management. We anticipate that in the future, additional sensor combinations will enable more accurate characterizations of health status, and consequently, treatments could be better tailored to improve the quality of life in patients.

Acknowledgements

This work was supported by the Hartwell Foundation Individual Biomedical Research Award and the Simons Foundation Autism Research Initiative—Explorer Award (#549099). M.A. was partially supported by the Postdoctoral Fellowship for Women Scientists from the Planning and Budgeting Committee, the Council for Higher Education, Israel.

Conflict of Interest

The authors declare no conflict of interest.

Keywords

autism, finger tapping test, flexible electronics, pressure sensors, spasticity

Received: June 30, 2019
Revised: September 10, 2019
Published online:

[1] H. Zeng, Y. Zhao, *Sensors* **2011**, *11*, 638.
[2] Y. Adesida, E. Papi, A. H. McGregor, *Sensors* **2019**, *19*, 1597.
[3] E. Valero, A. Sivanathan, F. Bosché, M. Abdel-Wahab, *Appl. Ergon.* **2016**, *54*, 120.
[4] M. Munoz-Organero, J. Parker, L. Powell, S. Mawson, M. Munoz-Organero, J. Parker, L. Powell, S. Mawson, *Sensors* **2016**, *16*, 1631.
[5] F. A. V. Porciuncula, Roto, D. Kumar , I. Davis, S. Roy, C. J. Walsh, L. N. Awad, *PM&R* **2018**, *10*, S220.
[6] L. Chan, M. Rodgers, H. Park, P. Bonato, S. Patel, *J. Neuroeng. Rehabil.* **2012**, *9*, 21.
[7] Q. W. Oung, H. Muthusamy, H. L. Lee, S. N. Basah, S. Yaacob, M. Sarillee, C. H. Lee, *Sensors* **2015**, *15*, 21710.
[8] Y. Moon, R. S. McGinnis, K. Seagers, R. W. Motl, N. Sheth, J. A. Wright, R. Ghaffari, J. J. Sosnoff, *PLoS One* **2017**, *12*, e0171346.
[9] J. Taylor, R. Kolamunnage-Dona, A. G. Marson, P. E. M. Smith, A. P. Aldenkamp, G. A. Baker, *Epilepsia* **2010**, *51*, 48.
[10] L. Chukoskie, J. Townsend, M. Westerfield, *Int. Rev. Neurobiol.* **2013**, *113*, 207.
[11] C.-Y. Pan, C.-H. Chu, C.-L. Tsai, M.-C. Sung, C.-Y. Huang, W.-Y. Ma, *Autism* **2017**, *21*, 190.
[12] J. F. M. Fleuren, G. E. Voerman, C. V. Erren-wolters, J. Snoek, J. S. Rietman, H. J. Hermens, A. V. Nene, *J. Neurol., Neurosurg. Psychiatry* **2010**, *81*, 46.
[13] A. A. Alhusaini, C. M. Dean, J. Crosbie, R. B. Shepherd, J. Lewis, *J. Child Neurol.* **2010**, *25*, 1242.
[14] S. Wang, J. Y. Oh, J. Xu, H. Tran, Z. Bao, *Acc. Chem. Res.* **2018**, *51*, 1033.
[15] Y. H. Lee, O. Y. Kweon, H. Kim, J. H. Yoo, S. G. Han, J. H. Oh, *J. Mater. Chem. C* **2018**, *6*, 8569.
[16] W. Gao, H. Ota, D. Kiriya, K. Takei, A. Javey, *Acc. Chem. Res.* **2019**, *52*, 523.
[17] T. Someya, M. Amagai, *Nat. Biotechnol.* **2019**, *37*, 382.
[18] Y. Khan, A. E. Ostfeld, C. M. Lochner, A. Pierre, A. C. Arias, *Adv. Mater.* **2016**, *28*, 4373.
[19] T. R. Ray, J. Choi, A. J. Bandodkar, S. Krishnan, P. Gutruf, L. Tian, R. Ghaffari, J. A. Rogers, *Chem. Rev.* **2019**, *119*, 5461.
[20] P. Jonnalagedda, F. Deng, K. Douglas, L. Chukoskie, M. Yip, T. N. Ng, T. Nguyen, A. Skalsky, H. Garudadri, *IEEE Healthcare Innovation Point-of-Care Technol. Conf.* **2016**, p. 167. Q7
[21] E. B. Brokaw, D. A. Heldman, R. J. Plott, E. J. Rapp, E. B. Montgomery, J. P. Giuffrida, in *2014 36th Annu. Int. Conf. IEEE Eng. Med. Biol. Soc., EMBC 2014*, IEEE, **2014**, pp. 4091–4094.
[22] J. A. Rogers, T. Someya, Y. Huang, *Science* **2010**, *327*, 1603.
[23] S. Sundaram, P. Kellnhofer, Y. Li, J. Y. Zhu, A. Torralba, W. Matusik, *Nature* **2019**, *569*, 698.
[24] D.-H. Kim, N. Lu, R. Ma, Y.-S. Kim, R.-H. Kim, S. Wang, J. Wu, S. M. Won, H. Tao, A. Islam, K. J. Yu, T. I. Kim, R. Chowdhury, M. Ying, L. Xu, M. Li, H. J. Chung, H. Keum, M. McCormick, P. Liu, Y. W. Zhang, F. G. Omenetto, Y. Huang, R. Coleman, J. A. Rogers, *Science* **2011**, *333*, 838.
[25] H. U. Chung, B. H. Kim, J. Y. Lee, J. Lee, Z. Xie, E. M. Ibler, K. Lee, A. Banks, J. Y. Jeong, J. Kim, C. Ogle, D. Grande, Y. Yu, H. Jang, P. Assem, D. Ryu, J. W. Kwak, M. Namkoong, J. B. Park, Y. Lee, D. H. Kim, A. Ryu, J. Jeong, K. You, B. Ji, Z. Liu, Q. Huo, X. Feng, Y. Deng, Y. Xu, K. I. Jang, J. Kim, Y. Zhang, R. Ghaffari, C. M. Rand, M. Schau, A. Hamvas, D. E. Weese-Meyer, Y. Huang, S. M. Lee, C. H. Lee, N. R. Shanbhag, A. S. Paller, S. Xu, J. A. Rogers, *Science* **2019**, *363*, eaau0780.
[26] S. Urry, *Meas. Sci. Technol.* **1999**, *10*, R16.
[27] A. H. Abdul Razak, A. Zayegh, R. K. Begg, Y. Wahab, A. H. Abdul Razak, A. Zayegh, R. K. Begg, Y. Wahab, *Sensors* **2012**, *12*, 9884.
[28] C. B. Cooper, K. Arutselvan, Y. Liu, D. Armstrong, Y. Lin, M. R. Khan, J. Genzer, M. D. Dickey, *Adv. Funct. Mater.* **2017**, *27*, 1605630.
[29] Y. Li, S. Luo, M. C. Yang, R. Liang, C. Zeng, *Adv. Funct. Mater.* **2016**, *26*, 2900.
[30] Y. Zhang, W. S. Kim, *Soft Rob.* **2014**, *1*, 132.
[31] Y. Yamamoto, S. Harada, D. Yamamoto, W. Honda, T. Arie, S. Akita, K. Takei, *Sci. Adv.* **2016**, *2*, e1601473.
[32] N. Luo, W. Dai, C. Li, Z. Zhou, L. Lu, C. C. Y. Poon, S. C. Chen, Y. Zhang, N. Zhao, *Adv. Funct. Mater.* **2016**, *26*, 1178.
[33] H.-H. Chou, A. Nguyen, A. Chortos, J. W. F. To, C. Lu, J. Mei, T. Kurosawa, W.-G. Bae, J. B.-H. Tok, Z. Bao, *Nat. Commun.* **2015**, *6*, 8011.
[34] Y. Ding, T. Xu, O. Onyilagha, H. Fong, Z. Zhu, B. Engineering Program, N. Program, *ACS Appl. Mater. Interfaces* **2019**, *11*, 6685.
[35] C.-L. Choong, M.-B. Shim, B.-S. Lee, S. Jeon, D.-S. Ko, T.-H. Kang, J. Bae, S. H. Lee, K.-E. Byun, J. Im, Y. J. Jeong, C. E. Park, J. J. Park, U. Chung, *Adv. Mater.* **2014**, *26*, 3451.
[36] B. C.-K. Tee, A. Chortos, A. Berndt, A. K. Nguyen, A. Tom, A. McGuire, Z. C. Lin, K. Tien, W.-G. Bae, H. Wang, P. Mei, H. H. Chou, B. Cui, K. Deisseroth, T. N. Ng, Z. Bao, *Science* **2015**, *350*, 313.
[37] B. Zhu, Y. Ling, L. Wei Yap, M. Yang, F. Lin, S. Gong, Y. Wang, T. An, Y. Zhao, W. Cheng, *ACS Appl. Mater. Interfaces* **2019**, *11*, 29014.
[38] S. Gong, W. Schwalb, Y. W. Wang, Y. Chen, Y. Tang, J. Si, B. Shirinzadeh, W. L. Cheng, *Nat. Commun.* **2014**, *5*, 3132.
[39] Y. Huang, X. Fan, S. Chen, N. Zhao, *Adv. Funct. Mater.* **2019**, *29*, 1808509.
[40] S. S. Lee, A. Reuveny, J. Reeder, S. S. Lee, H. Jin, Q. Liu, T. Yokota, T. Sekitani, T. Isoyama, Y. Abe, Z. Suo, T. Someya, *Nat. Nanotechnol.* **2016**, *11*, 472.
[41] X. Zhou, Y. Zhang, J. Yang, J. Li, S. Luo, D. Wei, *Nanomaterials* **2019**, *9*, 496.
[42] J. C. Yang, J.-O. Kim, J. Oh, S. Y. Kwon, J. Y. Sim, D. W. Kim, H. B. Choi, S. Park, *ACS Appl. Mater. Interfaces* **2019**, *11*, 19472.
[43] J. Shintake, E. Piskarev, S. H. Jeong, D. Floreano, *Adv. Mater. Technol.* **2018**, *3*, 1700284.
[44] D. J. Cohen, D. Mitra, K. Peterson, M. M. Maharbiz, *Nano Lett.* **2012**, *12*, 1821.
[45] Y. Zhai, J. Lee, Q. Hoang, D. Sievenpiper, H. Garudadri, T. N. Ng, *Flexible Printed Electron.* **2018**, *3*, 035006.
[46] B. You, C. J. Han, Y. Kim, B.-K. Ju, J.-W. Kim, *J. Mater. Chem. A* **2016**, *4*, 10435.
[47] J. Kim, T. N. Ng, W. S. Kim, *Appl. Phys. Lett.* **2012**, *101*, 103308.
[48] B. Y. Lee, J. Kim, H. Kim, C. Kim, S. D. Lee, *Sens. Actuators, A* **2016**, *240*, 103.
[49] S. Kang, J. Lee, S. Lee, S. G. Kim, J.-K. Kim, H. Algadi, S. Al-Sayari, D.-E. Kim, D. E. Kim, T. Lee, *Adv. Electron. Mater.* **2016**, *2*, 1600356. Q8
[50] S. Chen, B. Zhuo, X. Guo, *ACS Appl. Mater. Interfaces* **2016**, *8*, 20364.
[51] C. Metzger, E. Fleisch, J. Meyer, M. Dansachmuller, I. Graz, M. Kaltenbrunner, C. Keplinger, R. Schwodiauer, S. Bauer, *Appl. Phys. Lett.* **2008**, *92*, 013506.
[52] C. M. Boutry, M. Negre, M. Jorda, O. Vardoulis, A. Chortos, O. Khatib, Z. Bao, *Sci. Rob.* **2018**, *3*, eaau6914.

[53] X. Guo, Y. Huang, X. Cai, C. Liu, P. Liu, *Meas. Sci. Technol.* **2016**, *27*, 045105.
[54] J.-Y. Yoo, M.-H. Seo, J.-S. Lee, K.-W. Choi, M.-S. Jo, J.-B. Yoon, Industrial Grade, *Adv. Funct. Mater.* **2018**, *28*, 1804721.
[55] S. Takamatsu, T. Lonjaret, E. Ismailova, A. Masuda, T. Itoh, G. G. Malliaras, *Adv. Mater.* **2015**, *3*, 3.
[56] Y. Luo, J. Shao, S. Chen, X. Chen, H. Tian, X. Li, L. Wang, D. Wang, B. Lu, *ACS Appl. Mater. Interfaces* **2019**, *11*, 17796.
[57] F. R. Fan, W. Tang, Z. L. Wang, *Adv. Mater.* **2016**, *28*, 4283.
[58] B. Stadlober, M. Zirkl, M. Irimia-Vladu, *Chem. Soc. Rev.* **2019**, *48*, 1787.
[59] A. Shinde, P. Sahatiya, A. Kadu, S. Badhulika, *Flexible inted Electron.* **2019**, *4*, 025003.
[60] T. H. Ng, W. H. Liao, *J. Intell. Mater. Syst. Struct.* **2005**, *16*, 785.
[61] S. W. Thomas, S. J. Vella, M. D. Dickey, G. K. Kaufman, G. M. Whitesides, *J. Am. Chem. Soc.* **2009**, *131*, 8746.
[62] S. Niu, Y. Liu, X. Chen, S. Wang, Y. S. Zhou, L. Lin, Y. Xie, Z. L. Wang, *Nano Energy* **2015**, *12*, 760.
Q9 [63] J. Tao, R. Bao, X. Wang, Y. Peng, J. Li, S. Fu, C. Pan, Z. L. Wang, *Adv. Funct. Mater.* **2018**, 1806379.
[64] Y. Yang, H. Zhang, Z.-H. Lin, Y. S. Zhou, Q. Jing, Y. Su, J. Yang, J. Chen, C. Hu, Z. L. Wang, *ACS Nano* **2013**, *7*, 9213.
[65] K. Dong, Z. Wu, J. Deng, A. C. Wang, H. Zou, C. Chen, D. Hu, B. Gu, B. Sun, Z. L. Wang, *Adv. Mater.* **2018**, *30*, 1804944.
[66] M. S. Rasel, P. Maharjan, M. Salauddin, M. T. Rahman, H. O. Cho, J. W. Kim, J. Y. Park, *Nano Energy* **2018**, *49*, 603.
[67] S. Niu, Y. S. Zhou, S. Wang, Y. Liu, L. Lin, Y. Bando, Z. L. Wang, *Nano Energy* **2014**, *8*, 150.
[68] V. Sridhar, K. Takahata, *Sens. Actuators, A* **2009**, *155*, 58.
[69] X. Tang, Y. Miao, X. Chen, B. Nie, X. Tang, Y. Miao, X. Chen, B. Nie, *Sensors* **2019**, *19*, 2406.
[70] S. S. Mohan, M. D. M. Hershenson, S. P. Boyd, T. H. Lee, *IEEE J. Solid-State Circuits* **1999**, *34*, 1419.
[71] C.-I. Jang, K.-S. Shin, M. J. Kim, K.-S. Yun, K. H. Park, J. Y. Kang, S. H. Lee, *Appl. Phys. Lett.* **2016**, *108*, 103701.
Q10 [72] O. Ozioko, M. Hersh, R. Dahiya, *Proc. IEEE Sens.*, IEEE, **2018**, October, https://doi.org/10.1109/ICSENS.2018.8589826.
[73] B. Nie, R. Huang, T. Yao, Y. Zhang, Y. Miao, C. Liu, J. Liu, X. Chen, *Adv. Funct. Mater.* **2019**, *29*, 1808786.
Q11 [74] L. Y. Chen, B. C.-K. Tee, A. L. Chortos, G. Schwartz, V. Tse, D. J. Lipomi, H.-S. P. Wong, M. V. McConnell, Z. Bao, *Nat. Commun.* **2014**, *5*, 5028.
[75] A. N. Sokolov, B. C.-K. Tee, C. J. Bettinger, J. B.-H. Tok, Z. Bao, *Acc. Chem. Res.* **2012**, *45*, 361.
[76] N. T. Tien, T. Q. Trung, Y. G. Seoul, D. Il Kim, N.-E. Lee, *ACS Nano* **2011**, *5*, 7069.
[77] Z. Liu, Z. Yin, J. Wang, Q. Zheng, *Adv. Funct. Mater.* **2019**, *29*, 1806092.
[78] Q. Sun, D. H. Kim, S. S. Park, N. Y. Lee, Y. Zhang, J. H. Lee, K. Cho, J. H. Cho, *Adv. Mater.* **2014**, *26*, 4735.
[79] T. Someya, Y. Kato, T. Sekitani, S. Iba, Y. Noguchi, Y. Murase, H. Kawaguchi, T. Sakurai, *Proc. Natl. Acad. Sci. USA* **2005**, *102*, 12321.
[80] T. Sekitani, T. Someya, *Adv. Mater.* **2010**, *22*, 2228.
Q12 [81] T. N. Ng, M. L. Chabinyc, R. A. Street, A. Salleo, in *IEEE Int. Reliab. Phys. Symp.*, Phoenix, **2007**, pp. 243–247.
[82] T. N. Ng, J. H. Daniel, S. Sambandan, A.-C. Arias, M. L. Chabinyc, R. A. Street, *J. Appl. Phys.* **2008**, *103*, 044506.
[83] C. Liu, Y. Xu, Y. Noh, *Mater. Today* **2015**, *18*, 79.
[84] A. F. Paterson, S. Singh, K. J. Fallon, T. Hodsden, Y. Han, B. C. Schroeder, H. Bronstein, M. Heeney, I. Mcculloch, T. D. Anthopoulos, *Adv. Mater.* **2018**, *30*, 1801079.
[85] R. Ma, S. Y. Chou, Y. Xie, Q. Pei, *Chem. Soc. Rev.* **2019**, *48*, 1741.
[86] N. Matsuhisa, D. Inoue, P. Zalar, H. Jin, Y. Matsuba, A. Itoh, T. Yokota, D. Hashizume, T. Someya, *Nat. Mater.* **2017**, *16*, 834.
[87] A. J. Bandodkar, R. Nuñez-Flores, W. Jia, J. Wang, *Adv. Mater.* **2015**, *27*, 3060.
[88] M. D. Dickey, R. C. Chiechi, R. J. Larsen, E. A. Weiss, D. A. Weitz, G. M. Whitesides, *Adv. Funct. Mater.* **2008**, *18*, 1097.
[89] A. Hirsch, L. Dejace, H. O. Michaud, S. P. Lacour, *Acc. Chem. Res.* **2019**, *52*, 534.
[90] Y. Wang, C. Zhu, R. Pfattner, H. Yan, L. Jin, S. Chen, F. Molina-Lopez, F. Lissel, J. Liu, N. I. Rabiah, Z. Chen, J. W. Chung, C. Linder, M. F. Toney, B. Murmann, *Sci. Adv.* **2017**, *3*, e1602076.
[91] S. Xu, Z. Yan, K. Jang, W. Huang, H. Fu, J. Kim, Z. Wei, M. Flavin, J. Mccracken, R. Wang, A. Baeda, Y. Liu, D. Xiao, G. Zhou, J. Lee, H. U. Chung, H. Cheng, W. Ren, A. Banks, X. Li, U. Paik, R. G. Nuzzo, Y. Huang, Y. Zhang, J. A. Rogers, *Science* **2014**, *172*, 232.
[92] S. S. Mechael, Y. Wu, K. Schlingman, T. B. Carmichael, *Flexible Printed Electron.* **2018**, *3*, 043001.
[93] J. Yoon, Y. Jeong, H. Kim, S. Yoo, H. S. Jung, Y. Kim, Y. Hwang, Y. Hyun, W.-K. Hong, B. H. Lee, S. H. Choa, H. C. Ko, *Nat. Commun.* **2016**, *7*, 11477.
[94] J. Rivnay, S. Inal, A. Salleo, R. M. Owens, M. Berggren, G. G. Malliaras, *Nat. Rev. Mater.* **2018**, *3*, 17086.
[95] Y. Lee, T. W. Lee, *Acc. Chem. Res.* **2019**, *52*, 964.
[96] L. Cai, C. Wang, *Nanoscale Res. Lett.* **2015**, *10*, 320.
[97] J. S. Kim, K. Choi, B. Lee, Y. Kim, B. Hee Hong, *Annu. Rev. Mater. Res.* **2015**, *45*, 63.
[98] W. Zhu, S. Park, M. N. Yogeesh, D. Akinwande, *Flexible Printed Electron.* **2017**, *2*, 043001.
[99] J. Y. Oh, S. Rondeau-Gagné, Y. C. Chiu, A. Chortos, F. Lissel, G. J. N. Wang, B. C. Schroeder, T. Kurosawa, J. Lopez, T. Katsumata, J. Xu, C. Zhu, X. Gu, W. G. Bae, Y. Kim, L. Jin, J. W. Chung, J. B. H. Tok, Z. Bao, *Nature* **2016**, *539*, 411.
[100] Y. S. Zhang, A. Khademhosseini, *Science* **2017**, *356*, eaaf3627.
[101] R. E. Cohen, *Nature* **2018**, *562*, 48.
[102] R. A. Street, T. N. Ng, D. E. Schwartz, G. L. Whiting, J. P. Lu, R. D. Bringans, J. Veres, *Proc. IEEE* **2015**, *103*, 607.
[103] T. N. Ng, D. E. Schwartz, P. Mei, S. Kor, J. Veres, P. Bröms, C. Karlsson, *Flexible Printed Electron.* **2016**, *1*, 015002.
[104] A. F. Harper, P. J. Diemer, O. D. Jurchescu, *npj Flexible Electron.* **2019**, *3*, 11.
[105] G. Grau, J. Cen, H. Kang, R. Kitsomboonloha, W. J. Scheideler, V. Subramanian, *Flexible Printed Electron.* **2016**, *1*, 023002.
[106] K. N. Al-Milaji, R. R. Secondo, T. N. Ng, N. Kinsey, H. Zhao, *Adv. Mater. Interfaces* **2018**, *5*, 1701561.
[107] J. Chen, H. Liu, W. Wang, N. Nabulsi, W. Zhao, J. Y. Kim, M. Kwon, J. Ryou, *Adv. Funct. Mater.* **2019**, *29*, 1903162.
[108] Y. Guo, M. Zhong, Z. Fang, P. Wan, G. Yu, *Nano Lett.* **2019**, *19*, 1143.
[109] L. Gao, C. Zhu, L. Li, C. Zhang, J. Liu, H.-D. Yu, W. Huang, *ACS Appl. Mater. Interfaces* **2019**, *11*, 25034.
[110] E. J. Curry, K. Ke, M. T. Chorsi, K. S. Wrobel, A. N. Miller III, A. Patel, I. Kim, J. Feng, L. Yue, Q. Wu, C. L. Kuo, K. Lo, C. T. Laurencin, H. Ilies, R. K. Purohit, T. D. Nguyen, *Proc. Natl. Acad. Sci. USA* **2018**, *115*, 909.
[111] K. Xu, S. Li, S. Dong, S. Zhang, G. Pan, G. Wang, L. Shi, W. Guo, C. Yu, J. Luo, *Adv. Healthcare Mater.* **2019**, *8*, 1801649.
[112] T.-P. Huynh, P. Sonar, H. Haick, *Adv. Mater.* **2017**, *29*, 1604973.
[113] Y. Cao, Y. J. Tan, S. Li, W. W. Lee, H. Guo, Y. Cai, C. Wang, B. C.-K. Tee, *Nat. Electron.* **2019**, *2*, 75.
[114] J. Xu, G. Wang, Y. Wu, X. Ren, G. Gao, *ACS Appl. Mater. Interfaces* **2019**, *11*, 25613.
[115] T. Huynh, H. Haick, *Adv. Mater.* **2018**, *30*, 1802337.
[116] X. Chen, B. Assadsangabi, Y. Hsiang, K. Takahata, *Adv. Sci.* **2018**, *5*, 1700560.

[117] F. G. Carrasco, D. D. Alonso, L. Niño-de-Rivera, *Microelectron. Eng.* **2016**, *159*, 32.
[118] G.-Z. Chen, I.-S. Chan, D. C. C. Lam, *Sens. Actuators, A* **2013**, *203*, 112.
[119] K. Mansouri, R. N. Weinreb, J. H. Liu, *PLoS One* **2015**, *10*, 0125530.
[120] E. B. Papas, *Clin. Exp. Optom.* **2017**, *100*, 529.
[121] X. Fan, Y. Huang, X. Ding, N. Luo, C. Li, N. Zhao, S. C. Chen, *Adv. Funct. Mater.* **2018**, *28*, 1805045.
[122] G. Ge, Y. Zhang, J. Shao, W. Wang, W. Si, W. Huang, X. Dong, *Adv. Funct. Mater.* **2018**, *28*, 1802576.
[123] Y. Gao, H. Ota, E. W. Schaler, K. Chen, A. Zhao, W. Gao, H. M. Fahad, Y. Leng, A. Zheng, F. Xiong, C. Zhang, L. C. Tai, P. Zhao, R. S. Fearing, A. Javey, *Adv. Mater.* **2017**, *29*, 1701985.
[124] K. Denby, G. Nelson, C. A. Estrada, *J. Gen. Intern. Med.* **2013**, *28*, 1381.
[125] A. Muro-de-la-Herran, B. Garcia-Zapirain, A. Mendez-Zorrilla, A. Muro-de-la-Herran, B. Garcia-Zapirain, A. Mendez-Zorrilla, *Sensors* **2014**, *14*, 3362.
[126] S. Crea, M. Donati, S. De Rossi, C. Oddo, N. Vitiello, *Sensors* **2014**, *14*, 1073.
[127] H. Kato, T. Takada, T. Kawamura, N. Hotta, S. Torii, *Diabetes Res. Clin. Pract.* **1996**, *31*, 115.
[128] J. Kim, A. S. Campbell, B. Esteban-Fernandez de Avila, J. Wang, *Nat. Biotechnol.* **2019**, *37*, 389.
[129] M. Amit, R. K. Mishra, Q. Hoang, A. M. Galan, J. Wang, T. N. Ng, *Mater. Horiz.* **2019**, *6*, 604.
[130] K. Wang, U. Parekh, T. Pailla, H. Garudadri, V. Gilja, T. N. Ng, *Adv. Healthcare Mater.* **2017**, *6*, 1700552.
[131] Y. Khan, D. Han, A. Pierre, J. Ting, X. Wang, C. M. Lochner, G. Bovo, N. Yaacobi-Gross, C. Newsome, R. Wilson, A. C. Arias, *Proc. Natl. Acad. Sci. USA* **2018**, *115*, E11015.
[132] Z. Wu, W. Yao, A. E. London, J. D. Azoulay, T. N. Ng, *ACS Appl. Mater. Interfaces* **2017**, *9*, 1654.
[133] Z. Wu, Y. Zhai, H. Kim, J. D. Azoulay, T. N. Ng, *Acc. Chem. Res.* **2018**, *51*, 3144.
[134] A. Pierre, A. C. Arias, *Flexible Printed Electron.* **2016**, *1*, 043001.
[135] Z. Wu, W. Yao, A. E. London, J. D. Azoulay, T. N. Ng, *Adv. Funct. Mater.* **2018**, *28*, 1800391.
[136] Z. Wu, Y. Zhai, W. Yao, N. Eedugurala, S. Zhang, L. Huang, X. Gu, J. D. Azoulay, T. N. Ng, *Adv. Funct. Mater.* **2018**, *28*, 1805738.
[137] W. Yao, Z. Wu, E. Huang, L. Huang, A. E. London, Z. Liu, J. D. Azoulay, T. N. Ng, *ACS Appl. Electron. Mater.* **2019**, *1*, 660.
[138] T. Pfau, *J. Exp. Biol.* **2005**, *208*, 2503.
[139] H. Zhao, Z. Wang, *IEEE Sens. J.* **2012**, *12*, 943.
[140] S. Lydon, O. Healy, P. Reed, T. Mulhern, B. M. Hughes, M. S. Goodwin, *Dev. Neurorehabil.* **2014**, *8423*, 1.
[141] M. S. Goodwin, D. Erdoğmuş, S. Ioannidis, O. zdenizci, C. Cumpanasoiu, P. Tian, Y. Guo, A. Stedman, C. Peura, C. Mazefsky, M. Siegel, D. Erdogmus, S. Ioannidis, in *Int. Conf. Pervasive Comput. Technol. Healthcare*, **2018**, pp. 201–207. Q13
[142] D. Austin, J. McNames, K. Klein, H. Jimison, M. Pavel, *IEEE J. Biomed. Health Inf.* **2015**, *19*, 501.
[143] J. Son, A. Ra Ko, Y. H. Lee, Y. Kim, *Int. J. Precis. Eng. Manuf.* **2012**, *13*, 2083.
[144] T. L. Simmons, J. Snider, M. Amit, T. N. Ng, J. Townsend, L. Chukoskie, in *2019 9th Int. IEEE/EMBS Conf. Neural Eng. (NER)*, IEEE, **2019**, pp. 1042–1045. Q14
[145] E. Bremer, R. Balogh, M. Lloyd, *Autism* **2015**, *19*, 980.
[146] T. Duffield, H. Trontel, E. D. Bigler, A. Froehlich, M. B. Prigge, B. Travers, R. R. Green, A. N. Cariello, J. Cooperrider, J. Nielsen, A. Alexander, J. Anderson, P. T. Fletcher, N. Lange, B. Zielinski, J. Lainhart, *J. Clin. Exp. Neuropsychol.* **2013**, *35*, 867.
[147] P. Teitelbaum, O. Teitelbaum, J. Nye, J. Fryman, R. G. Maurer, *Proc. Natl. Acad. Sci. USA* **1998**, *95*, 13982.
[148] S. H. Koo, K. Gaul, S. Rivera, T. Pan, D. Fong, *Arch. Des. Res.* **2018**, *31*, 37.
[149] C. C. W. Yu, S. W. L. Wong, F. S. F. Lo, R. C. H. So, D. F. Y. Chan, *BMC Psychiatry* **2018**, *18*, 56.
[150] T. Rekand, *Acta Neurol. Scand.* **2010**, *122*, 62.
[151] The American Association of Neurological Surgeons. Spasticity. Q15
[152] A. J. Skalsky, P. B. Dalal, *Phys. Med. Rehabil. Clin. North Am.* **2015**, *26*, 21.
[153] P. Charalambous, P. A. Banaszkiewicz, D. F. Kader, *Interrate Reliability of a Modified Ashworth Scale of Muscle Spasticity*, **2014**. Q16
[154] D. M. Y. Poon, C. W. Y. Hui-Chan, *Dev. Med. Child Neurol.* **2009**, *51*, 128.
[155] B. J. E. Misgeld, M. Luken, D. Heitzmann, S. I. Wolf, S. Leonhardt, *IEEE J. Biomed. Health Inf.* **2016**, *20*, 748.
[156] J. Ferreira, V. Moreira, J. Machado, F. Soares, *2013 IEEE 3rd Port. Meet. Bioeng. (ENBENG)*, February **2013**, 1–4. Q17
[157] A. Jobin, M. F. Levin, *Dev. Med. Child Neurol.* **2000**, *42*, 531.
[158] X. Li, H. Shin, S. Li, P. Zhou, *Sci. Rep.* **2017**, *7*, 44022.
[159] L. Le-Ngoc, J. Janssen, *Rehabil. Med.* **2012**, 53. Q18
[160] N. Seth, D. Johnson, G. W. Taylor, O. B. Allen, H. A. Abdullah, *J. Neuroeng. Rehabil.* **2015**, *12*, 109.
[161] L. H. Sloot, L. Bar-On, M. M. van der Krogt, E. Aertbeliën, A. I. Buizer, K. Desloovere, J. Harlaar, *Dev. Med. Child Neurol.* **2017**, *59*, 145.
[162] S. Y. Song, Y. Pei, J. Liang, E. T. Hsiao-Wecksler, in *2017 Des. Med. Devices Conf.*, ASME, **2017**, p. V001T11A020. Q19
[163] S. Y. Song, Y. Pei, S. R. Tippett, D. Lamichhane, C. M. Zallek, E. T. Hsiao-Wecksler, in *2018 Des. Med. Devices Conf.*, ASME, **2018**, p. V001T10A007.
[164] P. D. Wettenschwiler, R. Stämpfli, S. Lorenzetti, S. J. Ferguson, R. M. Rossi, S. Annaheim, *Int. J. Ind. Ergon.* **2015**, *49*, 60.
[165] C. Trompetto, L. Marinelli, L. Mori, E. Pelosin, A. Curra, L. Molfetta, G. Abbruzzese, *Biomed. Res. Int.* **2014**, *2014*. Q20
[166] P. H. Lau, K. Takei, C. Wang, Y. Ju, J. Kim, Z. Yu, T. Takahashi, G. Cho, A. Javey, *Nano Lett.* **2013**, *13*, 3864.
[167] W. Zhu, M. N. Yogeesh, S. Yang, S. H. Aldave, J.-S. Kim, S. Sonde, L. Tao, N. Lu, D. Akinwande, *Nano Lett.* **2015**, *15*, 1883.
[168] A. Thibaut, C. Chatelle, E. Ziegler, M.-A. Bruno, S. Laureys, O. Gosseries, *Brain Inj.* **2013**, *27*, 1093.